

Understanding the Importance of Microphysics and Macrophysics for Warm Rain in Marine Low Clouds. Part I: Satellite Observations

TERENCE L. KUBAR, DENNIS L. HARTMANN, AND ROBERT WOOD

Department of Atmospheric Sciences, University of Washington, Seattle, Washington

(Manuscript received 9 January 2009, in final form 30 April 2009)

ABSTRACT

The importance of macrophysical variables [cloud thickness, liquid water path (LWP)] and microphysical variables (effective radius r_e , effective droplet concentration N_{eff}) on warm drizzle intensity and frequency across the tropics and subtropics is studied. In this first part of a two-part study, Moderate Resolution Imaging Spectroradiometer (MODIS) optical and *CloudSat* cloud radar data are used to understand warm rain in marine clouds. Part II uses simple heuristic models. Cloud-top height and LWP substantially increase as drizzle intensity increases. Droplet radius estimated from MODIS also increases with cloud radar reflectivity (dBZ) but levels off as dBZ > 0, except where the influence of continental pollution is present, in which case a monotonic increase of r_e with drizzle intensity occurs. Off the Asian coast and over the Gulf of Mexico, r_e values are smaller (by several μm) and N_{eff} values are larger compared to more remote marine regions. For heavy drizzle intensity, both r_e and N_{eff} values off the Asian coast and over the Gulf of Mexico approach r_e and N_{eff} values in more remote marine regions.

Drizzle frequency, defined as profiles in which maximum dBZ > -15, increases dramatically and nearly uniformly when cloud tops grow from 1 to 2 km. Drizzle frequencies exceed 90% in all regions when LWPs exceed 250 g m^{-2} and N_{eff} values are below 50 cm^{-3} , even in regions where drizzle occurs infrequently on the whole. The fact that the relationship among drizzle frequency, LWP, and N_{eff} is essentially the same for all regions suggests a near universality among tropical and subtropical regions.

1. Introduction

Warm oceanic clouds over the tropics and subtropics are extensive and important to the earth radiation balance, a result of their high albedo relative to the ocean surface (Hartmann and Short 1980; Slingo 1990). Single-layer marine stratiform water clouds cover nearly one-third of the global ocean surface (Charlson et al. 1987). The optical depth τ of a warm cloud is proportional to the cloud liquid water path (LWP) and inversely related to the cloud droplet effective radius r_e . The cloud LWP is generally considered a macrophysical variable that is controlled by both cloud-scale dynamics and the thermodynamics of the ambient air (Petty 2006). The effective radius, on the other hand, is the ratio of the third to second moments of the droplet size distribution and is predominantly a microphysical variable (Wood 2006b). If one assumes a lognormal size distribution that does

not vary in the vertical, then LWP itself is fundamentally related to both r_e and droplet concentration N_d (also a microphysical variable) as follows (e.g., Matrosov et al. 2004):

$$\text{LWP} = \left(\frac{4}{3}\right)\pi\rho N_d r_e^3 \exp(-3\sigma^2)\Delta h, \quad (1)$$

where σ is the distribution width and Δh the cloud thickness. Thus, for a given LWP, small changes in r_e are associated with substantial increases in N_d .

If one assumes that supersaturation is sufficient to activate all accumulation mode aerosols, then the aerosol number concentration is directly related to N_d . For marine clouds this is often a reasonable assumption (Martin et al. 1994; Miles et al. 2000). Regions influenced by continental aerosols and/or anthropogenic pollution tend to be characterized by higher N_d and smaller cloud droplet size (Han et al. 1994; Miles et al. 2000; Bréon et al. 2002; Bennartz 2007). For a given LWP, continental clouds thus tend to be brighter than pristine marine clouds [see Twomey (1974, 1977), whose results were confirmed observationally by Brenguier et al. (2000)]. As

Corresponding author address: Terence L. Kubar, Jet Propulsion Laboratory, MS 183-518, California Institute of Technology, 4800 Oak Grove Drive, Pasadena, CA 91109.
E-mail: terry.kubar@jpl.nasa.gov

a simple experiment to quantify the sensitivity of the radiative effect to changes in microphysics, Charlson et al. (1987) show that an increase in N_d of 30% (with LWP held fixed) results in a 10% reduction of r_e , which increases the solar albedo in the area covered by liquid marine stratiform clouds by 0.018 and enhances the global albedo by 0.005. This would account for a global average temperature decrease of -1.3 K, after accounting for feedback effects (Charlson et al. 1987). In an observational study over western and eastern Washington State of nonraining warm clouds, Hindman et al. (1977) found an inverse relationship between cloud droplet concentration and size. It is suggested that the presence of large concentrations of small cloud condensation nuclei (CCN) in western Washington during the study inhibited the production of large cloud droplets via coalescence. Other classical studies also suggest that high droplet concentrations are almost always observed in clouds that contain few, if any, large droplets (Squires 1956, 1958), but many of such studies do not quantify what “few” actually means.

In addition to the effect that droplet concentration has on the reflectivity of the cloud, droplet concentration also may be important in helping to determine the processes that form drizzle, such as collision and coalescence (Albrecht 1989). Collision efficiencies are reduced for smaller cloud drops (Rogers and Yau 1989). Albrecht (1989) proposes that an increase in N_d with a consequent decrease in r_e would decrease drizzle frequency and thus increase fractional cloudiness, enhancing cloud albedo. Measurements made during the First International Satellite Cloud Climatology Regional Experiment (FIRE) in horizontally homogeneous clouds in 1987 (400–500 km southwest of Los Angeles) not only demonstrate an inverse relationship between droplet size and reflected solar radiation but also show that the clouds with the lowest droplet concentrations have the highest propensity to drizzle significantly (Albrecht 1989). More recent studies by Pawlowska and Brenguier (2003), Comstock et al. (2004), vanZanten et al. (2005), and Wood (2005) quantify similar behavior. Drizzle also has the effect of scavenging CCN, and low CCN concentrations seem to be important for drizzle formation, suggestive of a positive feedback (Wood 2006a).

Many observational studies attempting to show the relative importance of both the large-scale meteorology (i.e., bulk thermodynamics) versus the microphysics (CCN and consequently droplet concentration) in the brightness and drizzle properties of warm clouds have used relatively small samples. The drizzle papers that examine the macrophysical and microphysical impacts are reviewed to some extent in Geoffroy et al. (2008). We wish to examine low cloud properties over the entire

tropical and subtropical Pacific and Gulf of Mexico utilizing collocated remote sensing instruments from the A-Train constellation (A-Train is described in Stephens et al. 2002). In this way, we shall relate the meteorology and variability of cloud macrophysics and microphysics with propensity of precipitation. We use the Moderate Resolution Imaging Spectroradiometer (MODIS) for cloud optical parameters r_e and τ and also the *CloudSat* Geometrical Profile (2B-GEOPROF) radar reflectivity profiles, from which we can not only infer cloud layers but also distinguish between drizzling and nondrizzling clouds.

The majority of the area that we examine in this study can be best characterized as a pristine marine environment, which we thus would expect to have quite low CCN and cloud droplet concentrations. Sufficient natural droplet concentration variability may still exist to examine the role of microphysics in warm cloud structure. Our region also encompasses areas potentially subject to the influence of continental aerosols, such as the Gulf of Mexico, and also off the eastern coast of Asia, so that different CCN regimes might be present in these areas, allowing for sufficient variability in our study. We will examine the importance of large-scale meteorology as well, as the tropics and subtropics are characterized by areas in which vertical cloud development is suppressed by pervasive strong low-level capping temperature inversions.

The objectives of this study are multifaceted, but include the following:

- documenting the variability of warm cloud macrophysical (cloud-top height, liquid water path) and microphysical (droplet size, concentration) properties across the tropics and subtropics;
- understanding the relative role of macrophysics and microphysics in drizzle intensity and frequency; and
- characterizing the relationship of drizzle frequency to cloud liquid water, droplet concentration, meteorological regimes, and, by inference, aerosol loadings

2. Data

a. MODIS

We use the narrow-swath MODIS/*Aqua* level-2 cloud subset along the *CloudSat* field-of-view track, the MAC06S0 product. The MODIS cloud data contain pixels whose horizontal resolution is either 1 or 5 km, and the narrow-swath data have an across-track width respectively of 11 km (eleven 1-km pixels) and 15 km (three 5-km pixels). All of the standard level-2 MODIS cloud products are contained within this narrow-swath subset, including cloud optical and physical parameters. We are

primarily concerned with the MODIS optical parameters for this study, including visible τ , effective radius r_e , and liquid water path. Because only τ and r_e are independent, we devote space to discussing the physical foundation for retrieval of these variables.

MODIS is a 36-band scanning spectroradiometer aboard *Aqua*, which is part of the A-Train constellation (Stephens et al. 2002). MODIS is sun-synchronous with equatorial crossing times of 1:30 a.m. and 1:30 p.m., but because we are interested in warm cloud optical properties we only use daytime retrievals. Four of the MODIS bands are used for the daytime shortwave cloud retrieval algorithm, including the visible band of $0.86 \mu\text{m}$ over the oceans ($0.65 \mu\text{m}$ over land), and 1.64 , 2.13 , and $3.75 \mu\text{m}$ in the near IR (King et al. 1997). The combination of one nonabsorbing visible band and one of the three absorbing near-IR bands is used to retrieve τ and r_e , respectively. In fact, cloud radiative properties depend nearly exclusively on both τ and r_e , making retrieval of these two parameters extremely relevant (Nakajima and King 1990). A detailed examination of MODIS retrievals can be found in King et al. (1997).

As mentioned, the three near-IR bands are 1.64 , 2.13 , and $3.75 \mu\text{m}$, and r_e is sensitive to a somewhat different cloud depth depending on the choice of band used, since longer wavelength bands are more strongly absorbing and thus will be absorbed more readily and hence closer to cloud top. The $3.75\text{-}\mu\text{m}$ band is most sensitive to drops in the uppermost one to two units of visible optical depth (Han et al. 1994). We use the r_e produced using the $3.75\text{-}\mu\text{m}$ channel to minimize problems associated with thin and broken clouds and to give an r_e that is most representative of cloud top (Nakajima and Nakajima 1995).

We also use MODIS to determine liquid water path as $LWP = 2\rho\tau r_e/3$ (King et al. 1997). As LWP is a post-processed MODIS variable, its horizontal resolution is 1 km, as for τ and r_e . We also use cloud-top temperature and cloud fraction, which are both 5-km variables, and are derived from bands in the thermal region (King et al. 1997). We only use scenes in which MODIS cloud-top temperatures (in conjunction with *CloudSat* cloud-top temperatures from ECMWF) are warmer than 273 K, since the focus of our study is warm clouds. To ensure some horizontal homogeneity, at least at the horizontal scale in question, we also require all MODIS pixels to have a cloud fraction of 1, which we discuss in greater detail in the methods section.

b. *CloudSat* radar reflectivity

CloudSat, which is the first satellite-borne cloud radar, has an operational frequency of 94 GHz, at which frequency the backscatter of clouds can be measured.

We use 12 total months of *CloudSat* and MODIS data from two boreal autumn and winter seasons, September 2006–February 2007 and September 2007–February 2008. Our results are insensitive to the months used. As part of the A-Train constellation, *CloudSat* closely follows *Aqua* MODIS (Stephens et al. 2002), allowing us to match this active sensor with the passive radiometer. *CloudSat* has a horizontal footprint of 1.7 km along track by 1.3 km across track, and an effective vertical resolution of 240 m (due to oversampling).

CloudSat has an operational sensitivity of -30 dBZ (where $\text{dBZ} = 10 \log_{10} Z$, with the formal definition of Z given in the next paragraph) which prevents some optically thin clouds from being seen. According to Fox and Illingworth (1997), a radar sensitivity threshold of -30 dBZ would detect 80%–90% of marine stratocumulus with LWPs between 1 and 20 g m^{-2} . The lowest LWP in our study with optically thin clouds already screened out is 18 g m^{-2} as given by MODIS. We use the 2B-GEOPROF *CloudSat* data, which contains profiles of radar reflectivity and cloud mask [see Mace (2007) for information regarding version 5.3 cloud mask]. We use the highest confidence detections of the *CloudSat* cloud mask to discriminate between cloudy and clear layers, in which a cloud is sensed when the reflectivity exceeds the *CloudSat* sensitivity. We save all values of reflectivity where clouds exist, after making a small correction for gaseous absorption, which is a standard *CloudSat* product. Because *CloudSat* is an active sensor, it can sense multiple cloud layers, and we ensure that all of our clouds are single layer because we are interested in the microphysical processes and drizzle characteristics of warm clouds. The vast majority (93%) of warm clouds sensed by *CloudSat* whose MODIS cloud fraction is 1 and for which $\tau > 3$ are single layered.

The size of the scatterers determines the magnitude of the radar reflectivity factor Z_E (e.g., Houze 1993). For the Rayleigh regime, when drop size is much smaller than the radar wavelength, Z_E is the sixth moment of the particle size distribution as follows (Fox and Illingworth 1997):

$$Z_E (\text{mm}^6 \text{ m}^{-3}) = \int_0^{\infty} N(D) D^6 dD, \quad (2)$$

in which $N(D)$ is the number concentration of drops with diameters between D and $D + dD$. We should note that because $D > 300 \mu\text{m}$, (2) is no longer valid as drops scatter in the Mie regime, so that very high reflectivities are not seen with *CloudSat*, putting a limit on maximum observable rain rates (Comstock et al. 2004; Stephens and Haynes 2007). The sixth power in (2) makes Z_E extremely sensitive to large drops, and in fact a small

number of drizzle-sized drops (i.e., $D \sim 200 \mu\text{m}$) would dominate the reflectivity while adding little to the cloud liquid water content (Fox and Illingworth 1997). Only one drizzle drop per liter with a diameter of $200 \mu\text{m}$ would have a reflectivity of -12 dBZ but an LWC of only 0.04 g m^{-3} (Fox and Illingworth 1997). Specifically, drizzle becomes important when it adds to the radar reflectivity to the same extent that the cloud droplet population does, such that the reflectivity is at least doubled (e.g., an increase of 3 dBZ ; Fox and Illingworth 1997). A reflectivity thresholding technique can distinguish between cloud profiles in which drizzle contribution to LWC is negligible from those in which drizzle becomes significant (Fox and Illingworth 1997; Matrosov et al. 2004). Using an 8.66-mm wavelength Doppler radar, Frisch et al. (1995) show that a -15-dBZ threshold effectively discriminates between drizzling and nondrizzling clouds. Other studies have used similar dBZ values to separate nonprecipitating from precipitating clouds (e.g., Comstock et al. 2004; Stephens and Haynes 2007; other studies are referenced in Liu et al. 2008). We designate all profiles with maximum dBZ greater than -15 dBZ as containing drizzling clouds.

c. ECMWF analysis profiles

European Centre for Medium-Range Weather Forecasts (ECMWF) profiles of temperature and pressure, which are available with the standard *CloudSat* products, have been integrated and collocated by the *CloudSat* team as an auxiliary set of variables, and we use these to ascertain cloud-top temperatures. We exclude all profiles with high thin clouds from our analysis to prevent possible cirrus contamination (which can be particularly problematic for retrievals of optical properties) and require that the highest *CloudSat* cloud layer corresponds to a temperature that is not colder than 273 K .

3. Methods

a. Collocation of MODIS and *CloudSat*

For τ , r_e , and LWP, which are 1-km pixels, we average all possible pixels of the 11 across *CloudSat* track by 5 pixels along *CloudSat* track (for a possible averaging of 55 pixels); and for the original 5-km pixels, we average all possible pixels of the three across the *CloudSat* track by the one pixel along track. This averaging technique provides a possible effective size of $11 \text{ km} \times 5 \text{ km}$ for τ , r_e , and LWP, and $15 \text{ km} \times 5 \text{ km}$ for cloud-top temperature and cloud fraction. All geolocation variables have an original horizontal resolution of 5 km. We do this so that all original 1-km and 5-km MODIS pixels are on a 5-km grid along the *CloudSat* orbital track.

The collocation of MODIS and *CloudSat* involves finding and averaging all aforementioned averaged MODIS assemblages that are located within 0.025° latitude and longitude and within 15 min of each *CloudSat* profile that actually detects a single-layer warm cloud, and averaging the MODIS variables if necessary. The vast majority of the time only one MODIS averaged quantity falls within these spatial and temporal conditions (92% of the cases), although occasionally two MODIS pixel sets are found because of the slight offset of the two instruments.

To reduce complications due to partially cloudy scenes at a scale that is no larger than 15 km across track by 10 km along track, the averaged MODIS cloud fraction is required to be 1. Also, to preclude any possible problems with optically thin clouds, we require that all original 1-km τ values must be at least 3, which are then averaged into the larger grid. We refer to these optical depth and cloud fraction requirements as the “solid and thick” criteria. Although our requirement of a cloud fraction of 1 and $\tau > 3$ biases our results toward low clouds that are more horizontally extensive and homogeneous and may exclude some small trade cumuli, it also helps reduce any optical property retrieval problems that may be associated with broken cloudiness. Also, while these requirements tend to bias against small open-cellular convection, which may be strongly drizzling, they are meant to create more of a level playing field for comparison of warm cloud properties among considerably different meteorological regimes. Of all the warm clouds sensed by MODIS within the *CloudSat* pixels, the requirements that *CloudSat* senses single-layer warm clouds and also that MODIS retrievals of optical depth be greater than three for *all* the individual MODIS pixels located within each MODIS assemblage allows us to retain 21% of all *CloudSat* pixels and MODIS assemblages. Our analysis for the entire study is based on this screening of warm clouds, and values and means of all quantities are reflections of this. In Fig. 1a, we present a map showing the fraction of MODIS warm cloud assemblages that meet the aforementioned MODIS solid and thick and *CloudSat* single-layer criteria. In the deep convective regions, the fraction is relatively small (15%–20%) owing to the ubiquity of trade cumuli there, which tend to be more patchy and inhomogeneous. Values are also fairly low in the far northeast (NE) Pacific and the far southeast (SE) Pacific, primarily because warm clouds tend to be very shallow there, and we disregard cloudy pixels in the lowest three gates (up to $\sim 720 \text{ m}$) because of potential near-surface clutter. To elucidate this point, in Fig. 1b we show the fraction of MODIS warm assemblages that meet the MODIS criteria, with no information about *CloudSat*, and generally this looks

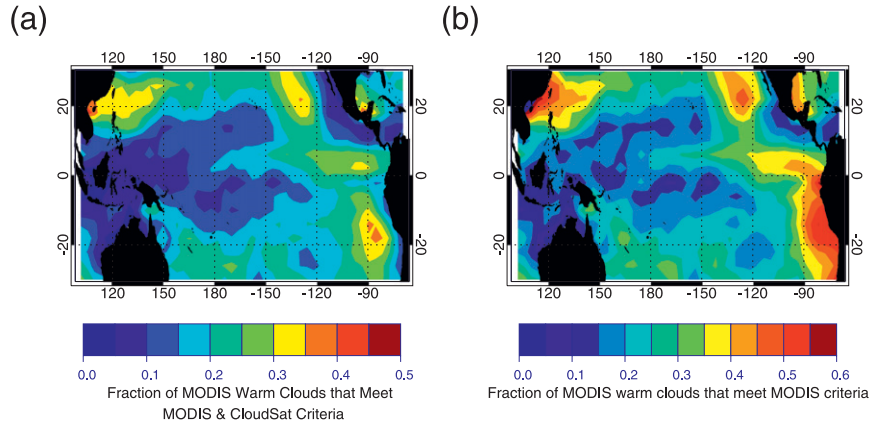


FIG. 1. (a) Fraction of MODIS warm clouds that *CloudSat* can sense that have $\tau > 3$ and a cloud fraction of 1 for all individual MODIS pixels, (b) fraction of MODIS warm clouds that have $\tau > 3$ and a cloud fraction of 1 for all individual MODIS pixels.

quite similar to Fig. 1a except for the aforementioned stratocumulus regions, suggesting that the clouds are solid and thick there but perhaps very shallow or otherwise not detected by *CloudSat*. Though not used in this study, preliminary Cloud–Aerosol Lidar and Infrared Pathfinder Satellite Observation (CALIPSO) analyses indicate that many stratocumulus clouds are missed by *CloudSat* when tops are below about 1 km.

b. Derived effective droplet concentration, N_{eff}

While MODIS mean r_e certainly conveys information about the mean size of the individual cloud droplets in the *uppermost* part of the cloud, the droplet concentration is equally important in describing the microphysical structure of a cloud. For a given cloud LWP, for instance, a small droplet size suggests a large droplet concentration, and vice versa. Droplet concentration is not retrieved by MODIS but can be derived with knowledge of both LWP and r_e . The expression for N_{eff} , known as effective droplet concentration, is given by Wood (2006b) (see also Brenguier et al. 2000; Szczodrak et al. 2001; Bennartz 2007) as

$$N_{\text{eff}} = \sqrt{2} B^3 \Gamma_{\text{eff}}^{1/2} \frac{\text{LWP}^{1/2}}{r_e^3}, \quad (3)$$

where $B = (\frac{3}{4}\pi\rho_w)^{1/3} = 0.0620$ and Γ_{eff} is the adiabatic rate of increase of liquid water content with respect to height. Three assumptions are that the liquid water content increases linearly with height above cloud base, that r_e refers to cloud top, and that r_e is equal to the geometric radius. The last assumption tends to be more inaccurate for drizzling clouds with broad drop size distributions, so N_{eff} may be an underestimate of N_d in such conditions. In (3), N_{eff} is only weakly dependent on

Γ_{eff} ; Γ_{eff} in turn is weakly dependent on pressure and temperature, for which we use the ECMWF analysis, and is also a function of an adiabaticity factor, which can range from zero to one. Few measurements exist of the adiabaticity factor, although it is often observed to be close to unity, particularly for nondrizzling stratocumulus clouds (Albrecht et al. 1990; Zuidema et al. 2005; Wood 2006b). In cumulus clouds, however, the adiabaticity factor can be significantly lower because of entrainment (Rauber et al. 2007). We use an adiabaticity factor of 1, which means we assume that the clouds are adiabatic.

We realize that an adiabatic assumption is a significant one, and consequently we have performed a sensitivity study to estimate a lower limit of the true N_{eff} . In Part II of this study, the adiabaticity factor is parameterized as $f_{\text{ad}} = z_0/(z_0 + z)$, where z_0 is a scaling parameter set to 500 m (see Wood et al. 2009, hereafter Part II) and z the height above cloud base. For the eight regions compared in this study (see section 5), the *subadiabatic* N_{eff} ranges from 45% of the *adiabatic* N_{eff} where clouds are geometrically thickest to 68% of the *adiabatic* N_{eff} where clouds are thinnest. These values represent lower limits because stratiform cloud bases are often above the LCL. We use an f_{ad} value of 1 because it makes fewer overall assumptions, given the uncertainties and complications in quantifying cloud subadiabaticity.

c. Regions of study

We use pixels for which the MODIS land/water flag indicates ocean, which restricts our analysis away from the immediate coast. We also restrict our study to tropical and subtropical latitudes from 30°S to 30°N (longitude range from 100°E to 70°W). We choose such regions because we are most interested in the role that the

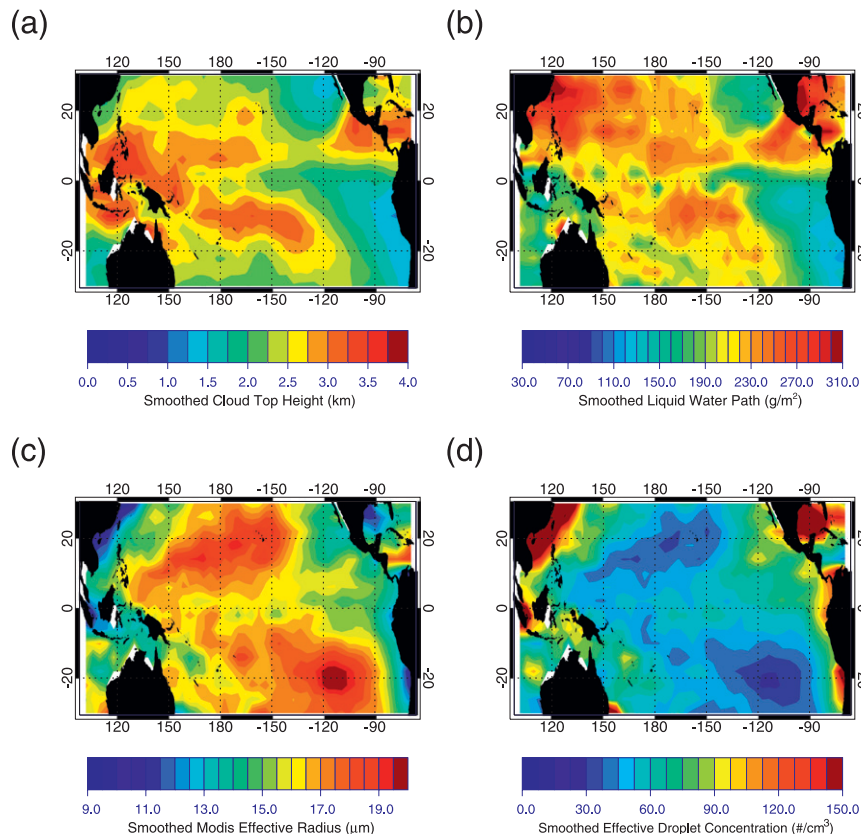


FIG. 2. (a) Smoothed warm cloud-top height (km), (b) liquid water path (g m^{-2}), (c) r_e (μm), and (d) N_{eff} (cm^{-3}). Cloud-top heights here and in all subsequent figures are from *CloudSat*.

natural variability of warm cloud macrophysics and microphysics may have on not only the cloud structure but also on drizzle frequency and intensity. A good portion of the area that we examine can be best characterized as a remote marine environment, which we thus would expect to have quite low CCN and correspondingly low cloud droplet concentrations, except for near the Asian coast and over the Gulf of Mexico.

4. Geographic distribution of warm cloud properties

We now present maps of various quantities that characterize the vertical structure, macrophysical, microphysical, and drizzling characteristics of warm clouds that are seen by both MODIS and *CloudSat*. We begin by looking at all screened warm clouds, regardless of whether our *CloudSat* test ($\text{dBZ}_{\text{MAX}} > -15$) indicates the clouds to be drizzling. Figure 2 contains maps of cloud-top height, LWP, r_e , and N_{eff} . Cloud-top heights in Fig. 1 and all subsequent figures and calculations are from *CloudSat*. These particular maps all contain 12 months of data and have been averaged into 4° latitude \times 4° longitude bins. For slightly better clarity,

these maps have been weakly smoothed with a 1–2–1 filter in the zonal direction to reduce noise. While most $4^\circ \times 4^\circ$ bins in our analysis contain at least several hundred screened warm clouds, and some a few thousand, a nonnegligible number of latitude–longitude bins contain only on the order of ~ 50 clouds. This is not surprising in some deep convective regions or in a few areas where the boundary layer top is very shallow (e.g., 500 m), so that low clouds there are missed by *CloudSat*.

Warm cloud-top heights tend to be high, even above 3 km, in regions associated with deeper convection. Even though we have screened out pixels containing overlying higher clouds via both MODIS and *CloudSat*, it is quite possible that these warm clouds are connected to larger, more organized deeper convective systems. In contrast, cloud-top heights tend to be quite low near the South American coast and extending west, and also near and offshore of the North American/Baja California coast. Regions of suppressed cloud tops tend to be collocated with high static stability (Fig. 3a) and cloud tops in general largely follow the structure of the underlying SST distribution (Fig. 3b). The cloud-top distribution is

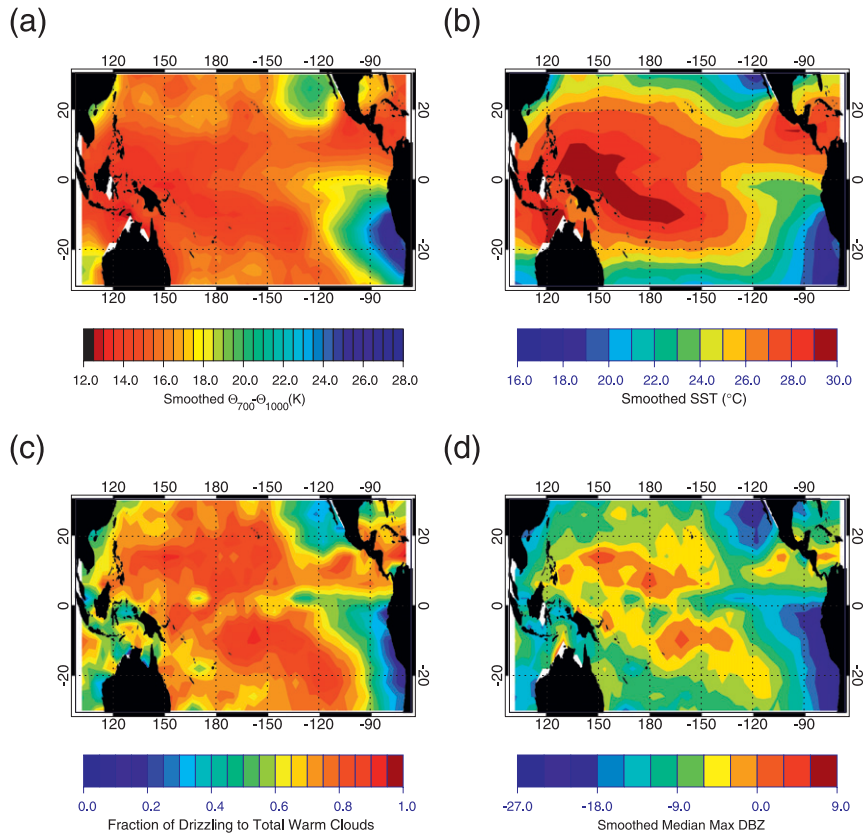


FIG. 3. (a) Smoothed 700–1000-mb $\Delta\theta$ (K), (b) smoothed SST ($^{\circ}\text{C}$), (c) fraction of drizzling to screened warm clouds, and (d) median max dBZ.

consistent with our understanding of the factors controlling marine boundary layer (MBL) depth (Riehl et al. 1951; Neibuherger et al. 1961; Bretherton and Wyant 1997), including observations (Wood and Bretherton 2004; Wu et al. 2008).

Maps of LWP in Fig. 2b tend to show patterns generally similar to those of the cloud height maps, which should be expected for the most part because the cloud height is likely a good indicator of cloud thickness (at least given a relatively constant cloud base height), so that a thicker cloud should contain more liquid water. Some differences exist, however, namely that LWP is especially high (approaching 300 g m^{-2} or more on average) off the coast of Asia near $\sim 120^{\circ}\text{E}$ and also over the Gulf of Mexico, even though cloud tops are not necessarily highest in these regions. It is possible that this can be partly explained by the very large droplet concentrations near the Asian coast and in the Gulf of Mexico (Fig. 2d). It is also possible that the presence of overlying aerosols would tend to result in a slight underestimation of LWP in the more polluted regimes, although based on the Wilcox et al. (2009) study the LWP underestimate is likely less than 20 g m^{-2} even in

the presence of absorbing pollution aerosols. The areas off the coast of Asia and over the Gulf of Mexico are likely influenced by continental aerosols and pollution, which tend to be dominated by smaller droplets and higher CCN concentrations. In fact, we see the inverse relationship between r_e and N_{eff} quite nicely when examining Figs. 2c and 2d, which show that variability in r_e is largely associated with N_{eff} . We also note that in much of the remote tropics and subtropics away from continents, droplet radius is quite large ($r_e > 15\text{ }\mu\text{m}$) and N_{eff} is quite low ($< 60\text{ cm}^{-3}$). Proximity to land areas tends to be important for both particle size and droplet concentration. The average geographic correlation coefficient between r_e and N_{eff} for each of the $9^{\circ} \times 6^{\circ}$ boxes (map not shown) is -0.83 .

We are also interested in understanding some of the background meteorology that may be responsible for controlling both the macrophysical and microphysical properties of warm clouds. We use the lower tropospheric stability (LTS), defined as $\Theta_{700\text{mb}} - \Theta_{1000\text{mb}}$ (Klein and Hartmann 1993) in Fig. 3a, which has been calculated by using the collocated ECMWF temperature profiles where both MODIS and *CloudSat* indicate that

single-layer warm clouds are present. Small values are indicative of regions with either weak temperature inversions or infrequent inversions. This is the case over most of the domain, with notable exceptions being the equatorial cold tongue and far southeastern Pacific, as well the northeastern Pacific. As mentioned, low cloud tops are collocated with high static stability, consistent with Wood and Bretherton (2004), who find that the marine boundary layer depth is negatively correlated with LTS over the NE and SE Pacific.

Figure 3c shows the fraction of drizzling to screened warm clouds (nondrizzling and drizzling) and has very similar spatial structure to both the LTS and SST structures. Finally, Fig. 3d shows the median dBZ of the screened warm clouds and looks similar spatially, as we would expect, to the drizzling warm cloud fraction. In fact, by definition, warm clouds that drizzle more than 50% of the time must have a median dBZ > -15 , and vice versa. More screened warm clouds than not are drizzling across the majority of the tropics and subtropics, with the exceptions being the areas already discussed. The pervasiveness of drizzle across the tropics and subtropics has also been pointed out by Suzuki and Stephens (2008) using *CloudSat* data, and Leon et al. (2008) have also used *CloudSat* and CALIPSO to survey drizzle frequency and intensity. It should also be emphasized again that our identification of drizzling clouds does not guarantee that drizzle reaches the surface, but rather that drizzle-sized drops are contained in the warm clouds. As the radar reflectivity increases above -15 dBZ, however, we would expect that a larger probability of these drops actually reach the surface. Figure 4 in Comstock et al. (2004) shows dBZ profiles of “light” (dBZ_{MAX} of -15) and “heavy” drizzle (dBZ_{MAX} of 0), in which drizzle reaches the surface for the heavy drizzle cases. Results examining drizzle that reaches the surface are also discussed in vanZanten et al. (2005) and Wood (2005). Further investigation of evaporation of drizzle below cloud base is beyond the scope of this study.

What macro- and microphysical differences are there between drizzling and nondrizzling clouds? Our Fig. 4 shows the mean difference of drizzling versus nondrizzling clouds of cloud-top height, LWP, r_e , and N_{eff} , now in 6° latitude \times 9° longitude boxes (larger boxes than in Fig. 2 to help ensure reasonable statistics). In most areas, drizzling clouds are deeper than nondrizzling clouds, and in some regions, especially in areas of frequent deep convection, this difference is more than 1 km. While the difference is positive almost everywhere, it is quite small particularly in regions where the mean cloud-top height is low, such as the marine stratocumulus regions (see Fig. 2a). In many of these areas,

warm clouds are less likely to drizzle than not, and even when they do drizzle, drizzle rates are very weak. As we shall see later, cloud-top heights tend to increase with dBZ, and where dBZ differences between drizzling and nondrizzling clouds are small, we would also expect cloud-top height differences to be small.

The LWP of drizzling clouds is larger than the LWP of nondrizzling clouds everywhere, and the LWP difference is quite large everywhere, even in the aforementioned regions where the warm clouds are very shallow. This seems to suggest that the propensity to form drizzle is limited by the availability of cloud water, arguing for the importance of macrophysics to warm rain. It is interesting to note that in the far west Pacific (near and just south of the equator), the LWP of drizzling clouds is not all that different from the LWP of nondrizzling clouds. These are regions where the screened warm cloud drizzling frequency is high and the mean LWP is also high.

Figure 4c shows the difference of mean particle size of drizzling versus nondrizzling clouds. Generally, the r_e of drizzling clouds is several microns larger than that of nondrizzling clouds. Some increase in r_e would be expected by LWP alone, since deeper clouds allow more condensational growth. In some regions, namely around 20°S from about 120° to 90°W and also in regions near and poleward of 20°N , the difference approaches about $5\ \mu\text{m}$. The fact that r_e is almost always larger in drizzling clouds is consistent with the notion that since r_e represents the mean particle size near cloud top, a shift to larger droplets would imply that a larger percentage of droplets within the entire distribution of the cloud would have a greater potential of growing to become drizzle or even rain drops, particularly since coalescence growth is more effective for larger drops.

Figure 4d shows the difference of N_{eff} of drizzling versus nondrizzling warm clouds. Drizzling clouds generally have somewhat lower concentrations, but in many regions, the differences are quite modest, on the order of only about $10\text{--}20\ \text{cm}^{-3}$. Exceptions to this include California and Mexico where drizzling clouds have considerably lower droplet concentrations versus nondrizzling clouds. This may suggest that in regions of relatively high background number concentrations, warm rain formation effectively removes smaller droplets via collision and coalescence. Alternatively, lower number concentrations may be more conducive for drizzle, and in regions frequently impacted by higher concentrations, drizzling concentrations should be considerably lower.

We now have a sense that both cloud microphysics and macrophysics may be different in drizzling versus nondrizzling clouds, but we are also interested in the relative sensitivity of drizzle rate to both changes in

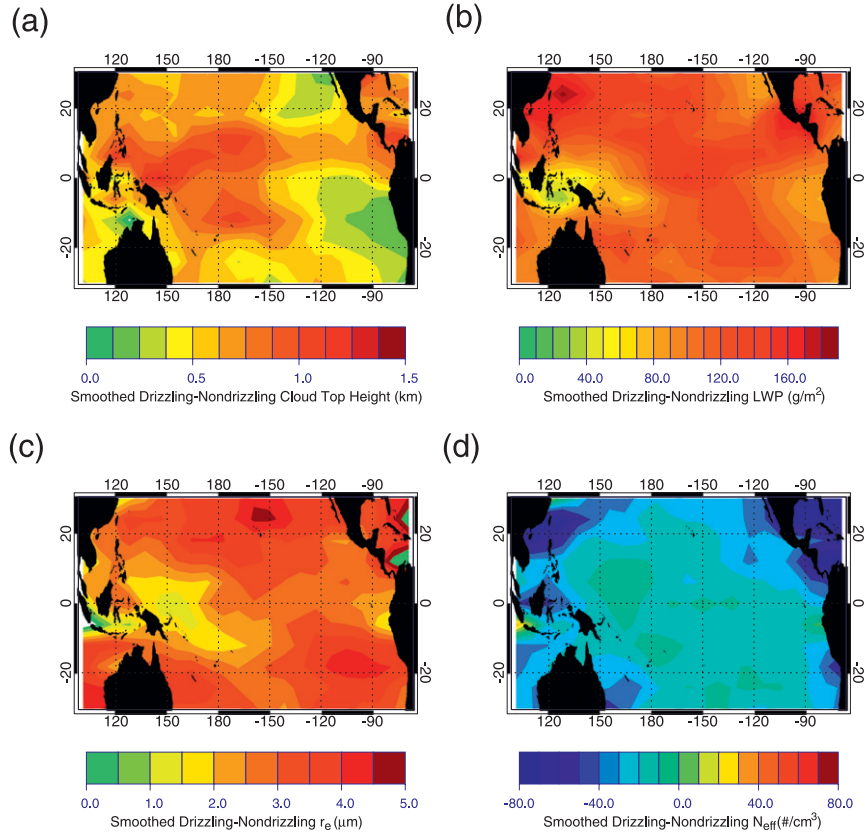


FIG. 4. Mean differences in drizzling and nondrizzling clouds for (a) cloud-top height (km), (b) LWP (g m^{-2}), (c) r_e (μm), and (d) N_{eff} (cm^{-3}).

LWP (macrophysics) and N_{eff} (microphysics) for the drizzling cloud population only. To quantify this, in each 6° latitude \times 9° longitude box, we calculate the mean LWP and N_{eff} where the radar reflectivity is larger than the median drizzling reflectivity for each geographic box and where the radar reflectivity is smaller than the median drizzling reflectivity. For reference, we also present ΔdBZ as an indicator of how much the precipitation changes. Figure 5 gives us a sense of the fractional change in both LWP and N_{eff} (i.e., $\Delta\text{LWP}/\text{LWP}$ and $\Delta N_{\text{eff}}/N_{\text{eff}}$). The mean value of $\Delta\text{LWP}/\text{LWP}$ is 0.41. The values of $\Delta\text{LWP}/\text{LWP}$ tend to be particularly large in parts of the North Pacific, along the equator, and the southeastern Pacific. On the other hand, in Fig. 5b, which shows $\Delta N_{\text{eff}}/N_{\text{eff}}$, we see that fractional changes of droplet concentrations are quite small (mean value of -0.10). If we instead assume that f_{ad} decreases with cloud depth (see section 3b), $\Delta N_{\text{eff}}/N_{\text{eff}}$ becomes somewhat more negative (not shown) because cloud thickness increases with drizzle intensity, which decreases the adiabaticity factor and thus N_{eff} . Nonetheless, by assuming adiabatic clouds, larger negative values of $\Delta N_{\text{eff}}/N_{\text{eff}}$ are still present over the Gulf of Mexico, the

far northeast Pacific, and off the coast of Asia, which are also the areas that show larger N_{eff} differences between drizzling and nondrizzling clouds. These results suggest that changes in the intensity of drizzle are much more sensitive to changes in LWP than to changes in N_{eff} . Alternatively, a cloud that is already precipitating has a considerably larger change in its liquid water than its droplet concentration as drizzle intensity increases. Thus, once drizzle has begun, the macrophysics may be more important for drizzle intensity.

5. PDFs of cloud top, LWP, r_e , and N_{eff} versus dBZ for different regions

Based on the aforementioned horizontal distribution of warm cloud characteristics, we divide the data into eight regions, which are illustrated in Fig. 6. These include the 1) Asian coast, 2) Gulf of Mexico, 3) NE Pacific, 4) far NE Pacific, 5) SE Pacific, 6) far SE Pacific, 7) ITCZ and South Pacific convergence zone (SPCZ), and 8) equatorial cold tongue. Since these regions are quite large and since our analysis period is 12 months, the sample size of screened warm clouds is large (ranging

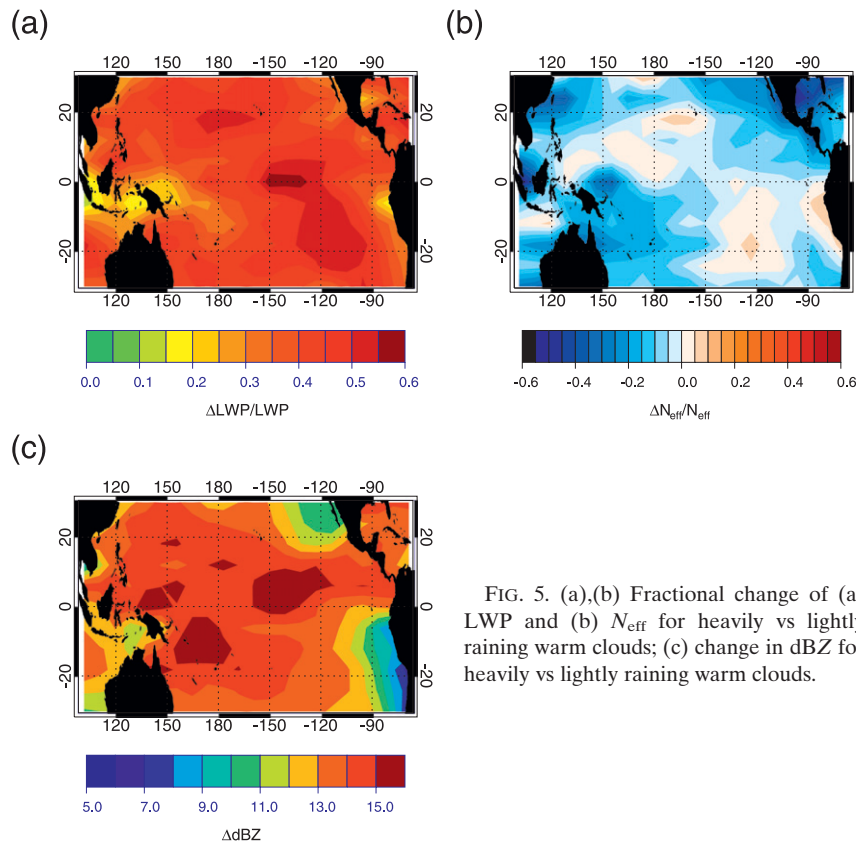


FIG. 5. (a),(b) Fractional change of (a) LWP and (b) N_{eff} for heavily vs lightly raining warm clouds; (c) change in dBZ for heavily vs lightly raining warm clouds.

from over 7000 over the Gulf of Mexico to over 56 000 over the NE Pacific), enhancing confidence in our results.

To synthesize the information from the maps presented in Fig. 2 for each of the eight regions, median values of cloud-top height, LWP, r_e , and N_{eff} are presented in Table 1. The fraction of MODIS warm clouds that meet the aforementioned MODIS and *CloudSat* criteria is also shown in each of the regions, as is the actual number of screened warm clouds. We also present various drizzling characteristics, including the fraction of occurrence in which dBZ_{MAX} exceeds various dBZ thresholds and median dBZ_{MAX} above various thresholds. The rationale of our choice of the eight regions becomes more evident from Table 1, including that the Asian coast and Gulf of Mexico are characterized by considerably higher droplet concentrations, likely owing to the proximity of continental regions. Most of the open Pacific, on the other hand, is characterized by very low N_{eff} . Cloud droplet size in the SE Pacific, ITCZ and SPCZ, and NE Pacific is especially large. The far SE Pacific and far NE Pacific both have on average very shallow warm clouds, owing to frequent and strong low-level inversions there. In contrast, the ITCZ and SPCZ are characterized by deep warm clouds with

a high drizzling frequency (83.7%) and high median dBZ (0.1).

Based on geographical differences in meteorology and the macrophysical and microphysical differences in warm clouds, we wish to more closely examine how variables representing these change as a function of dBZ. To do this, nondrizzling clouds are first separated from drizzling clouds. Then, the 25th, 50th, and 75th percentiles of reflectivity are determined in each region for the drizzling population only. This ensures an equal number of samples for a particular region in each drizzling category (0–25th, 25th–50th, 50–75th, 75th–100th), although because the drizzling frequency is quite variable from region to region, regions with a very low drizzling frequency (i.e., the far SE Pacific) have many more samples in the nondrizzling category compared to each of the drizzling categories.

Figure 7 shows the SE Pacific probability distribution functions (PDFs) of cloud-top height, LWP, r_e , and N_{eff} for the aforementioned dBZ categories, and also for the nondrizzling population. We perform the calculations for all eight regions but only show the SE Pacific in Fig. 7 and the Asian coast in Fig. 8 to illustrate differences between a remote, clean marine environment and one influenced by continental aerosols and pollution. We

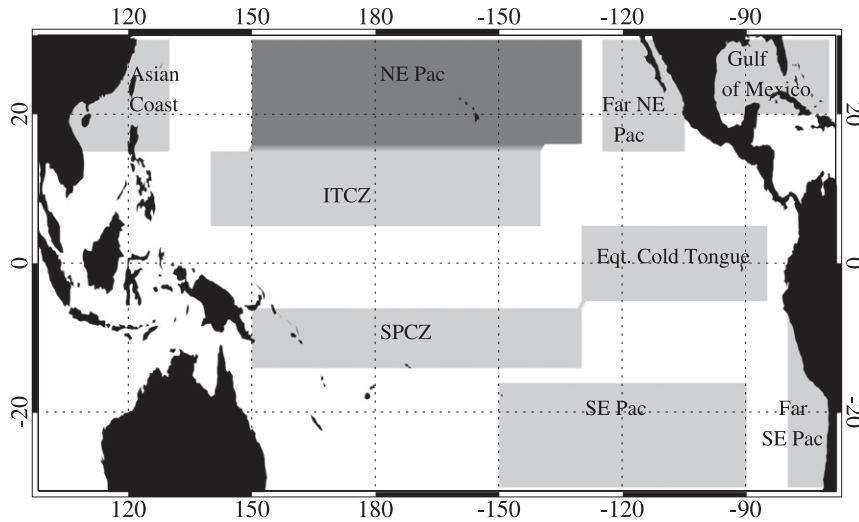


FIG. 6. Locations of eight regions. All pixels flagged by MODIS as coastal regions are excluded from analysis.

also note that the SE Pacific looks similar to most of the other remote marine regions, particularly the ITCZ/SPCZ and NE Pacific, and that the Asian coast is similar to the Gulf of Mexico.

In Fig. 7, we see that both the cloud-top height and LWP peaks shift toward higher values as backscatter increases. The PDFs also tend to spread out with more drizzle. Increasing cloud top and LWP with reflectivity suggests, not surprisingly, that these two macrophysical quantities are quite related to one another, such that clouds grow vertically and thus contain more liquid water when more drizzle is produced.

Turning to Fig. 7c, we see that the r_e peak increases from nondrizzling clouds to the lightest drizzling cate-

gory, but then other r_e categories for stronger drizzle look similar to one another, peaking at a higher particle size than nondrizzling or very lightly drizzling clouds. This suggests that mean droplet size near cloud top is less related to amount of drizzle, especially if drizzle already is happening. Cloud-top height and LWP appear to be more coupled with drizzle intensity than r_e or N_{eff} .

Finally, in Fig. 7d, we see that all the N_{eff} distributions look rather similar irrespective of dBZ, except that the nondrizzling population is shifted toward somewhat higher values. We will discuss this more thoroughly in upcoming sections, but it appears that the microphysical changes are more evident at the onset of drizzle than for changes in drizzle intensity. This suggests that increased

TABLE 1. Parameters indicating the macrophysical and microphysical cloud properties and drizzle characteristics for each of the eight regions. Bold numbers represent the maximum value among all regions, and italics represent minimum values. All numerical values other than percentages represent median values for each region below row two.

	NE Pacific	Far NE Pacific	Gulf of Mexico	Asian coast	SE Pacific	Far SE Pacific	ITCZ/SPCZ	Equatorial cold tongue
(%) of MODIS warm clouds that meet criteria	21.6	16.9	19.1	30.2	20.9	18.4	<i>13.4</i>	22.5
No. of MODIS warm clouds that meet criteria	56 238	10 908	<i>7074</i>	20 837	46 967	12 601	24 556	40 697
Cloud-top height (km)	2.0	1.4	2.3	2.2	2.1	<i>1.3</i>	2.7	1.7
LWP (g m^{-2})	177	138	250	263	161	<i>108</i>	216	155
r_e (μm)	16.7	13.9	12.2	<i>11.5</i>	18.0	13.2	17.1	14.6
N_{eff} (cm^{-3})	44	71	127	159	33	72	44	61
(%) with dBZ > -15	69.7	38.1	63.9	61.9	72.5	<i>23.0</i>	83.7	55.7
(%) with dBZ > 0	27.5	7.4	27.7	26.9	28.4	2.3	50.3	18.6
(%) with dBZ > 7.5	11.2	2.0	10.8	9.9	10.6	<i>0.3</i>	28.6	7.0
dBZ for all clouds	-8.4	-18.4	-9.0	-10.1	-7.6	-22	0.1	-13.4
dBZ for dBZ > -15	-2.9	-8.1	-1.9	-1.8	-2.8	<i>-10.0</i>	3.2	-5.0
dBZ for dBZ > 0	6.2	4.5	6.0	5.8	5.8	3.4	8.5	5.7

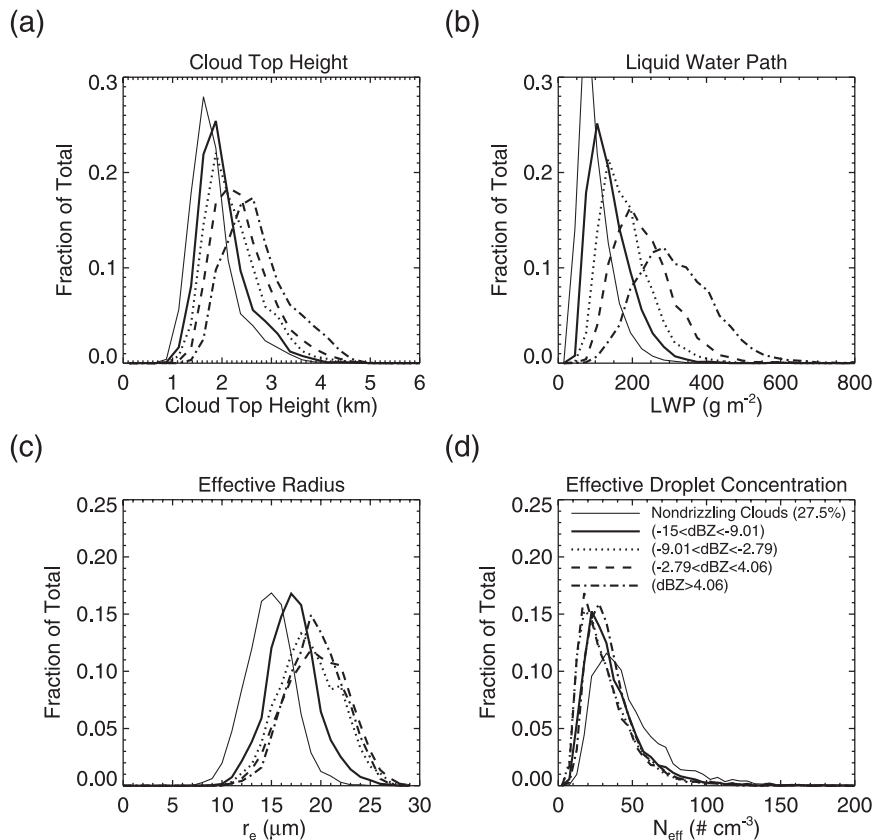


FIG. 7. PDFs of (a) cloud-top height, (b) LWP, (c) r_e , and (d) N_{eff} for the SE Pacific for nondrizzling and drizzling dBZ quartiles; dBZ ranges for each drizzling category are given, as is the nondrizzling cloud frequency.

r_e with drizzle is largely a result of greater vertical cloud development rather than changes in microphysics (N_{eff}) per se.

Figure 8 shows analogous PDFs, but for the Asian coast. It is apparent that cloud-top height and LWP both increase with dBZ. One difference, however, is that a large number of clouds have LWP values that surpass 600 g m^{-2} , especially for the two highest dBZ categories. Also, the LWP distributions tend to be less peaked for the Asian coast, especially as dBZ increases. Particle size, while certainly increasing with dBZ, tends to be much smaller near the Asian coast compared to the SE Pacific. Distributions of N_{eff} reveal great variability for the Asian coast, and many clouds have much larger droplet concentrations than the SE Pacific, with many concentrations surpassing 400 cm^{-3} . Smaller particle sizes and higher concentrations are likely due to the continental aerosol influence in this region. The highest drizzling category has a peak at lower concentrations, which may suggest either that heavy drizzle removes a large number of smaller particles, or perhaps that a lower droplet concentration simply increases precipitation. Assuming

instead an adiabaticity factor that reduces with cloud height leads to a more accentuated peak in low N_{eff} values at high drizzle intensity (not shown). We will explore these notions more in depth in the coming sections.

6. DBZ relationships for different regions

We now wish to synthesize the pertinent information from the PDFs presented in the previous section to better understand how universal cloud macro- or microphysical relationships are as a function of drizzle. By examining the median values, we can also more easily compare all eight regions.

Figure 9 presents median cloud-top height and LWP versus maximum dBZ for each of the eight regions. The reflectivity categories have been chosen as described in the previous section. The drizzling frequency is indicated in the legend of Fig. 9a, which is highest in the ITCZ and SPCZ at 84.3% and lowest in the Far SE Pacific at only 23%. Also, 95% confidence intervals are shown, although we only show them for two regions with the expected largest intervals: the far SE Pacific because

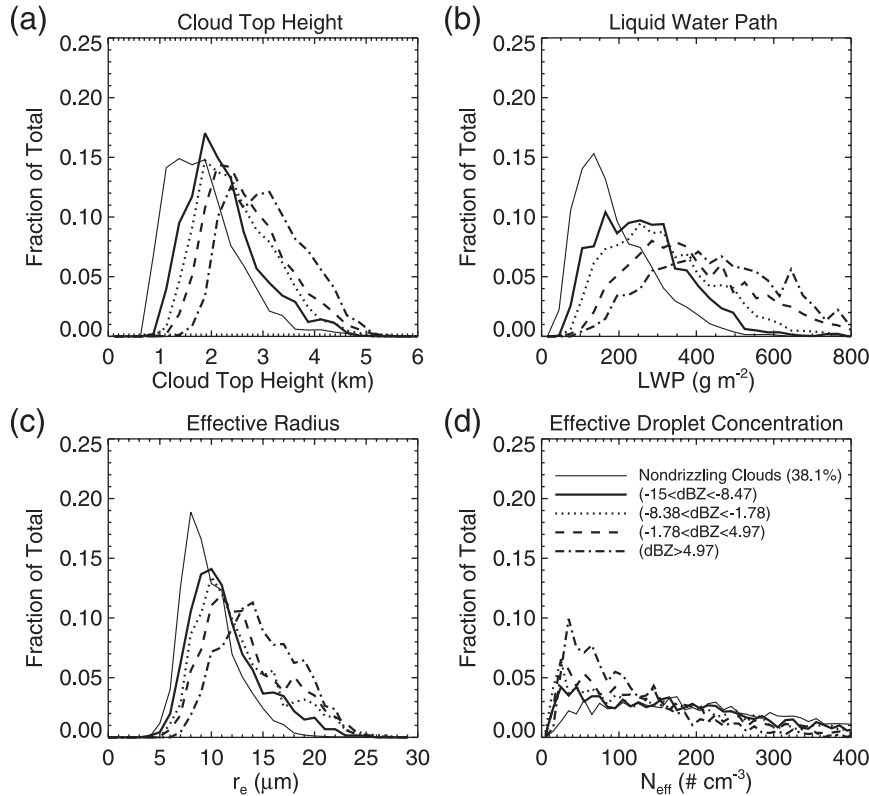


FIG. 8. As in Fig. 7, but for the Asian coast.

of its low drizzling frequency and thus smaller drizzling sample size and also the Gulf of Mexico, which contains quite a lot of microphysical variability, owing perhaps to its proximity to continental aerosols. We note that the confidence intervals even in these regions are narrow, so that curves separated visually are statistically distinct as well.

Figure 9a shows that cloud-top height increases as radar reflectivity increases, although there are certainly height differences among the different regions. When the reflectivity exceeds -15 dBZ, the reflectivity is linearly proportional to drizzle rate [see Comstock et al. (2004) for Z - R relationships] and thus we can consider the x axis as such. In the deep convective regions (ITCZ and SPCZ), warm clouds are approximately 1 km deeper for a given dBZ compared to the greatly suppressed far SE Pacific. We also note that median cloud tops grow to ~ 3.5 km in the ITCZ and SPCZ for large dBZ values, certainly suggestive of the convective nature of some of these deeper warm clouds. In Kubar and Hartmann (2008), a strong increase of precipitation rate occurs with cloud-top height, particularly for deep convective clouds. Similarly, we see that thicker warm clouds tend to be associated with greater drizzle. Cloud-top height alone, however, is not a good predictor of drizzle

intensity, as the relationships are quite different among the regions.

Figure 9b clearly shows that LWP increases in all regions with dBZ. Some regions, such as the ITCZ and SPCZ and NE Pacific, show over a threefold increase in LWP for nondrizzling clouds to the most heavily drizzling clouds, from about 100 g m^{-2} to over 300 g m^{-2} . The Asian coast and Gulf of Mexico stand out as having a considerably larger LWP for a given drizzle intensity compared to all the other regions, suggesting that more liquid water is needed in these regions, which have smaller mean radii and larger droplet concentrations, to produce a given amount of drizzle. When many small droplets are present, a greater microphysical barrier to precipitation may exist, as suggested by Albrecht (1989).

Figure 10 is analogous to Fig. 9, except for mean r_e and N_{eff} . Particle size increases with dBZ, although certainly significant differences exist among different regions, suggesting that r_e alone is not a particularly useful indicator of drizzle intensity. The SE Pacific, for instance, stands out as having the largest droplet size for a given dBZ, and in fact r_e is 5 - $8 \mu\text{m}$ larger for a given amount of drizzle in the SE Pacific compared to the Asian coast. Most regions tend to show a fairly sharp increase of r_e

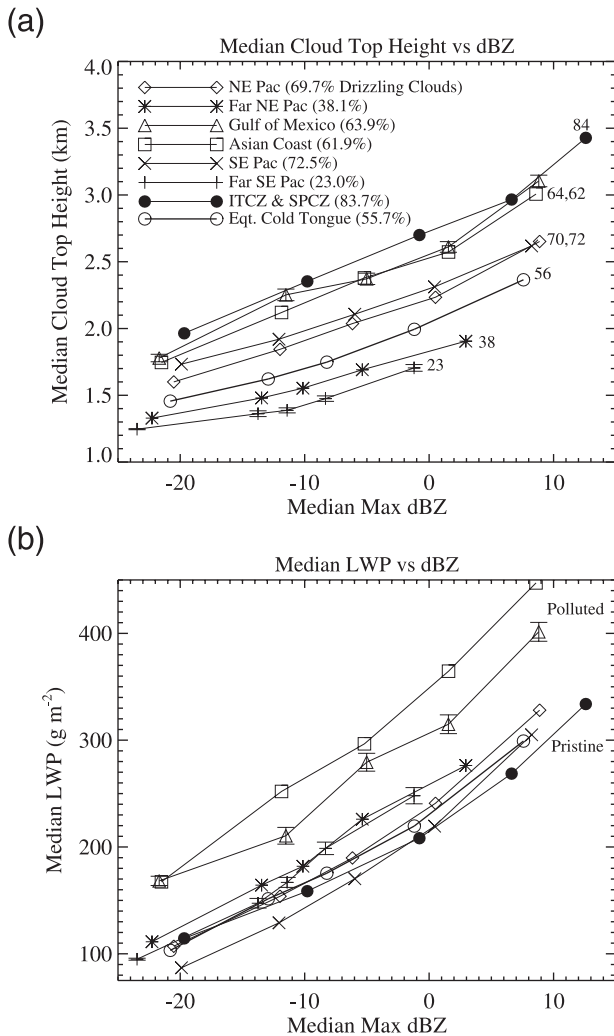


FIG. 9. (a) Median cloud-top height and (b) median LWP vs median maximum dBZ for each of the eight regions. In (a), numbers/percentages indicate frequency of drizzling warm clouds in each region. Note that 95% confidence intervals are shown for Gulf of Mexico and far SE Pacific.

with dBZ, followed by a leveling off toward higher reflectivity values, particularly as $\text{dBZ}_{\text{MAX}} > 0$. This suggests that the particle size near cloud top is a less important determining factor of drizzle intensity than integrated cloud liquid. The leveling off of r_e with reflectivity is not seen for either the Asian coast or Gulf of Mexico, and in fact mean r_e increases by $6 \mu\text{m}$ for non-drizzling warm clouds to the most heavily drizzling ones over the Gulf of Mexico.

Figure 10b shows the N_{eff} -dBZ relationships for all eight regions and, similar to the r_e -dBZ curves, the Asian coast and Gulf of Mexico stand out as regions with N_{eff} strongly decreasing with increasing dBZ. As we might expect from the maps presented earlier, non-

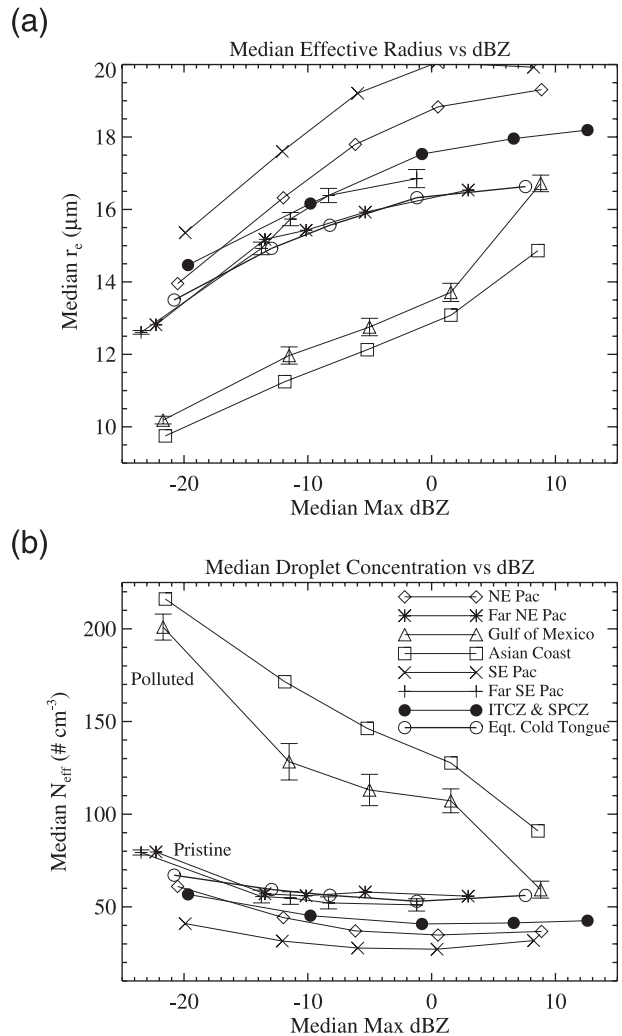


FIG. 10. As in Fig. 9, but for r_e and N_{eff} .

drizzling clouds near both the Asian coast and over the Gulf of Mexico have much higher number concentrations (more than 100 cm^{-3} larger than the other regions), highlighting perhaps the much higher concentrations expected in areas influenced by continental aerosols compared to remote marine regions. We also observe that aside from the Asian coast and Gulf of Mexico, N_{eff} changes very little with dBZ, especially once clouds are drizzling. As dBZ approaches 10, r_e and N_{eff} in the polluted regions approach values in cleaner regions. In much of the tropics and subtropics well removed from continental aerosols, the microphysics has perhaps some effect in determining the likelihood of drizzle but very little impact, if any, in regulating drizzle intensity. Warm cloud microphysics tends to play a much greater role in determining drizzle intensity for both the Asian coast and Gulf of Mexico. Thus, once drizzle has begun, the

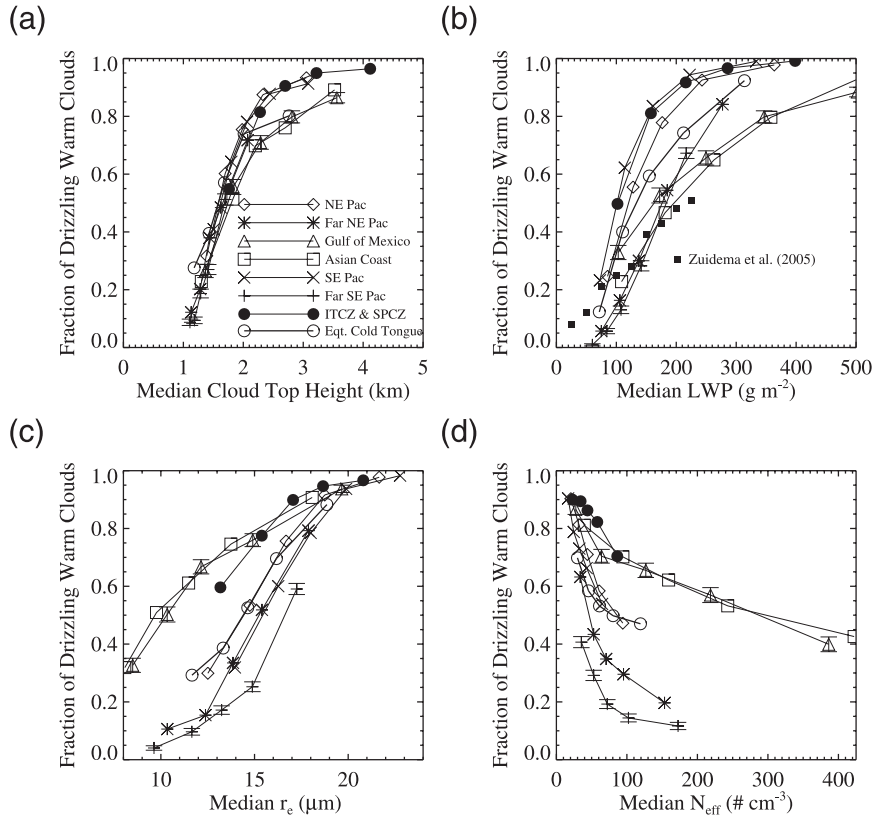


FIG. 11. Fraction of drizzling clouds for each region vs (a) cloud-top height, (b) LWP, (c) r_e , and (d) N_{eff} . As in Figs. 9 and 10, 95% confidence intervals are shown for the Gulf of Mexico and far SE Pacific. In (b), results shown from Zuidema et al. (2005) at 20°S, 85°W.

macrophysics may be more important for drizzle intensity. Part II of this study examines the theoretical basis for this behavior.

7. Drizzle probability

We attempt now to examine drizzle probability as a function of cloud top, LWP, r_e , and N_{eff} . Although a desirable objective would be to isolate the importance of each of these variables in quantifying how they relate to drizzle, this is not feasible given the lack of independence among these four variables. Nonetheless, understanding drizzle probability as a function of each variable sheds additional light on processes that may control warm rain.

Figure 11 contains four panels that show the frequency of drizzling clouds for cloud top, LWP, r_e , and N_{eff} categories. The five categories for each region include the 0th–20th, 20th–40th, 40th–60th, 60th–80th, and 80th–100th percentiles for each variable, and the frequency is simply the number of drizzling profiles divided by the total number of screened warm cloud profiles that

are bounded by each category. This method ensures an equal number of samples for a particular region for each of the five categories. As an example for the equatorial cold tongue, 59% of warm clouds are drizzling when the LWP is between 132 and 181 g m^{-2} (median value of 155 g m^{-2}), but 92% are drizzling when the LWP > 251 g m^{-2} (median value of 80th–100th LWP percentiles is 314 g m^{-2}). We also show 95% confidence intervals once again for only the far SE Pacific and the Gulf of Mexico, in which the standard error is given by $\sqrt{p(1-p)/N}$, where p in this case is the probability of drizzle and N the total number of profiles within a given variable range (i.e., LWP).

Starting with Fig. 11a, we see that drizzle frequency increases dramatically with cloud-top height in all areas, and in fact the relationship appears to be very tight, particularly when cloud-top height is less than 2 km. In regions where cloud tops are higher than 2 km, the frequency of drizzle is greater than 80% in most regions, except for the Asian coast, Gulf of Mexico, and equatorial cold tongue, where values are slightly lower. As cloud tops ascend to over 3 km, the probability of drizzle

is between 90% and 100% in regions where clouds can get this high. Cloud-top height alone thus reveals much information about drizzle frequency, consistent with Stephens et al. (2008).

The drizzle frequency plot versus LWP looks fairly similar to that of cloud top in that drizzle frequency increases dramatically with LWP, although there is somewhat more spread among the different regions. Despite the spread, which is likely because of varying microphysical regimes, the clear increase of drizzle occurrence with LWP is consistent with Fig. 9 in Leon et al. (2008), although that particular figure restricted r_e to between 19 and 22 μm (we have no size restriction in our Fig. 11b). In our study, clouds with a much higher LWP of $\sim 350 \text{ g m}^{-2}$ for the Asian coast and Gulf of Mexico compared to the LWP over the ITCZ and SPCZ, NE Pacific, and SE Pacific ($\sim 150 \text{ g m}^{-2}$) have the same drizzle frequency of about 0.8. Even though we are now looking at whether or not a cloud will drizzle, as opposed to the drizzle intensity as in the previous section, clouds near the Asian coast and over the Gulf of Mexico contain more liquid water for the same drizzle frequency as other regions.

The range of drizzle frequency versus LWP is impressive for the equatorial cold tongue, starting at only 0.12 for LWP $< 100 \text{ g m}^{-2}$ and increasing to 0.92 when LWP $> 300 \text{ g m}^{-2}$, indicative of the importance of LWP and drizzle formation there. Also noteworthy is the far SE Pacific, whose overall drizzle frequency is 0.23, where the drizzle frequency ranges from 0.0 when LWP is approximately 50 g m^{-2} to 0.67 as LWP approaches 200 g m^{-2} . Drizzle frequency versus LWP from Zuidema et al. (2005) (with drizzle defined as $\text{dBZ}_{\text{MAX}} > -17$ in that study) near 20°S , 85°W , an area within our far SE Pacific, is also shown in Fig. 11b. Drizzle frequencies are similar to the far SE Pacific, although somewhat lower particularly for higher LWPs. In our study, drizzle becomes much more likely even in the far SE Pacific for more favorable macrophysical conditions, but those conditions happen rather seldom, especially compared to most of our other regions. The macrophysics alone can thus very much be a limiting factor in whether or not a cloud will rain.

Figure 11c shows the drizzle frequency versus r_e , and as we might expect, drizzle becomes more common with increasing droplet radius. Since r_e is quite variable for our selected regions, however, it is not surprising to see the amount of spread in the curves. For instance, warm clouds with smaller r_e by several μm near the Asian coast and over the Gulf of Mexico tend to drizzle as frequently as clouds in other regions. As mean droplet size near cloud top gets larger, especially above 18 μm , warm clouds in all regions are very likely to be drizzling

(>0.9 frequency). It is also interesting to note that for a given r_e , variability in drizzle frequency seems to be related to LWP variability. For instance, for an r_e of 15 μm , the drizzling frequency in the far SE Pacific is only about 0.25, a region where LWPs are lowest, compared to a drizzling frequency of 0.7 for the Asian Coast, Gulf of Mexico, and ITCZ/SPCZ for the same r_e , where median LWPs are over twice as large (refer to Table 1). Thus the use of a fixed value of r_e such as 15 μm to infer drizzle presence, as is done in such studies as Jensen et al. (2008), may not be appropriate unless cloud LWP variations are small.

Figure 11d shows the drizzle frequency versus N_{eff} , and generally the probability of drizzle decreases with increasing droplet concentration. However, the range in drizzle frequency as a function of N_{eff} tends to be smaller for any particular region, indicating that microphysics alone is not as important as cloud-top height or LWP in controlling growth into drizzle-sized drops. In the ITCZ and SPCZ, for instance, drizzle frequency decreases only from 0.9 to 0.7 across the entire droplet concentration spectrum in those regions, compared to the drizzle frequency of 0.5 for small LWP to nearly 1.0 for large LWPs in that region. Although drizzle frequency tends to decrease as N_{eff} increases, the microphysics seem somewhat less important compared to cloud thickness or LWP for drizzle probability.

8. Macrophysical versus microphysical controls on drizzle frequency

Instead of trying to isolate the effect of individual variables on the likelihood that a nonfreezing cloud will drizzle, we now combine a macrophysical quantity (LWP) with a microphysical variable (N_{eff}) to better understand which conditions provide the most favorable conditions for drizzle. We can also make a better attempt to hold either the cloud microphysics or macrophysics constant in order to determine the extent to which we see at least part of the Albrecht (1989) effect, which suggests that regions of low CCN tend to provide more favorable environments for drizzle formation for a given cloud thickness or LWP. We should note that Leon et al. (2008) also explored similar relationships of drizzle frequency as a function of macrophysical and microphysical properties, although they used LWP and r_e rather than LWP and N_{eff} as in this study.

To understand microphysical and macrophysical controls on drizzle, we have produced contour plots of drizzle frequency as a function of both N_{eff} and LWP for each of the eight areas. Ten deciles of both N_{eff} and LWP are first computed, and then the drizzle frequency is calculated in each of the 100 categories. The fact that we use two

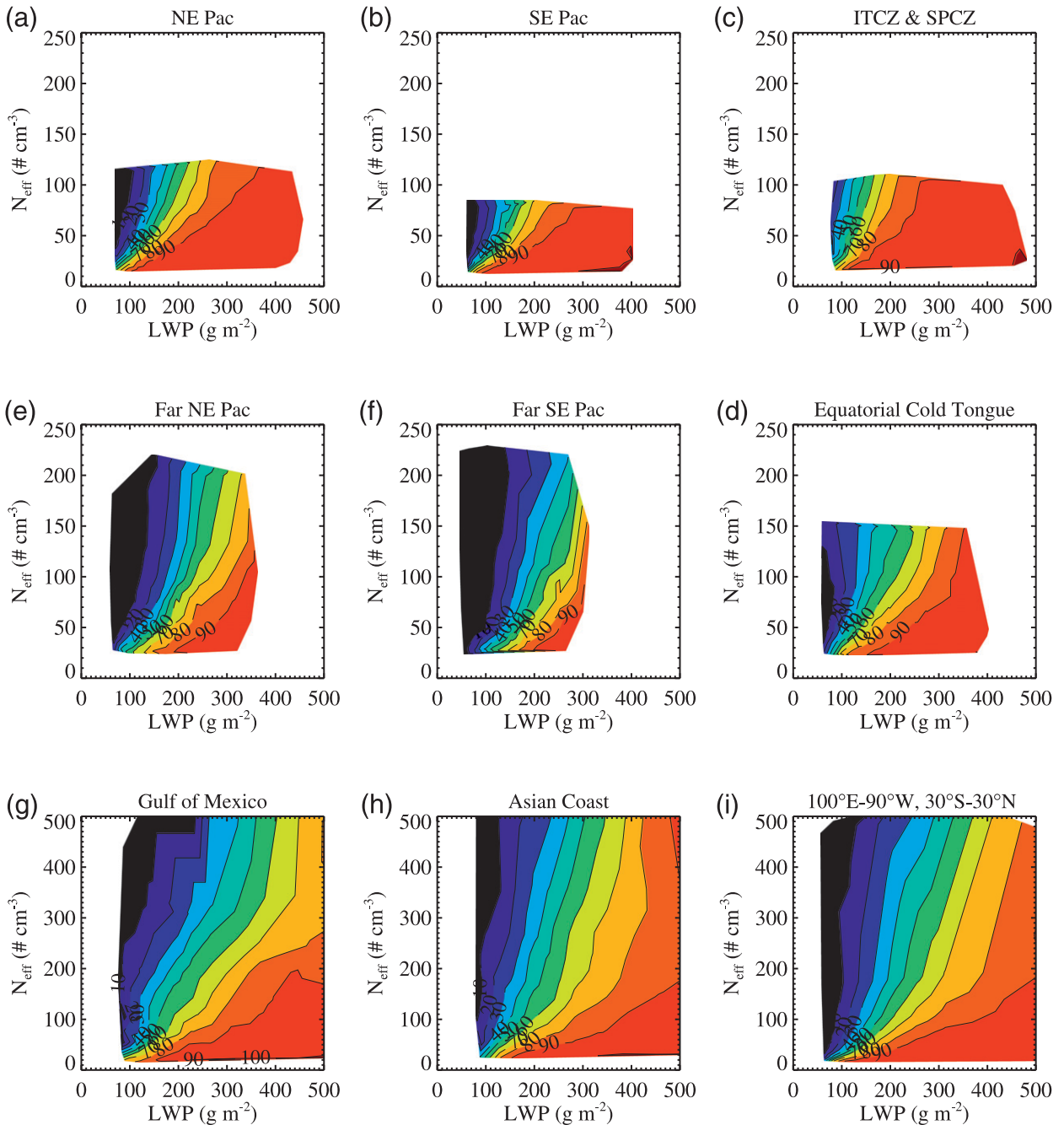


FIG. 12. Contours of drizzle frequency (% , from 0% to 100%) as a function of N_{eff} and LWP for (a) NE Pacific, (b) SE Pacific, (c) ITCZ and SPCZ, (d) equatorial cold tongue, (e) far NE Pacific, (f) far SE Pacific, (g) Gulf of Mexico, (h) Asian Coast, and (i) entire domain.

simultaneous variables for the categories precludes an equal number of observations in each bin, but this is unavoidable for this exercise.

Figure 12 shows contour plots of drizzle frequency versus N_{eff} and LWP for all eight regions and also for the entire domain. The contour lines are labeled accordingly, and each line is a 10% change in drizzle frequency,

ranging from 0% to 100%. Coincidentally, the top three contour plots are regions of low N_{eff} regions (NE Pacific, SE Pacific, ITCZ/SPCZ), the middle three moderate N_{eff} regions (far NE Pacific, far SE Pacific, equatorial cold tongue), and the bottom ones high N_{eff} regions (Gulf of Mexico, Asian coast). In all regions, we see that as N_{eff} is held constant, drizzle frequency steadily

increases with LWP. Additionally, as LWP is held constant, the likelihood of drizzle tends to decrease with increasing N_{eff} , which is thus consistent with part of the Albrecht (1989) effect. Unfortunately, with our satellite-borne observing system, we *cannot* assess whether cloud lifetime or fractional cloudiness changes with changes in N_{eff} . As LWP becomes sufficiently large in any region, the higher droplet concentration is less an inhibiting factor, and drizzle frequency becomes greater than 90%. It is also interesting that in the far SE Pacific, which is a region where warm clouds on average seldom drizzle, drizzle frequency can still be very likely (>90%) if N_{eff} is small enough (<50 cm^{-3}) and LWP is large enough (>200 g m^{-2}). The fact that the 90% contour is seen in all regions gives a sense of universality of drizzle sensitivity to both the macrophysics and microphysics. Qualitatively, warm clouds with high liquid water and lower number concentration are most likely to drizzle in any region.

Some other characteristics about Fig. 12 are worth mentioning for clarity. Except for the plots of the Asian coast, Gulf of Mexico, and entire domain, we have maintained the same x and y axes so that the contoured regions provide a sense of the actual range of both LWP and N_{eff} for a particular region. The Asian coast and Gulf of Mexico have a much larger N_{eff} range. For instance, the contour of drizzle frequency rarely surpasses N_{eff} values of 80 cm^{-3} in the SE Pacific, and the ninth N_{eff} decile is only 65 cm^{-3} , illustrative of a remote marine environment well removed from continental aerosols and pollution, whereas in the Gulf of Mexico the ninth N_{eff} decile is 386 cm^{-3} and N_{eff} can surpass 600 cm^{-3} (2.3% of the time). Also, the LWP in the far SE Pacific only exceeds 300 g m^{-2} about 3% of the time but does so 38% of the time over the Gulf of Mexico. We get a sense that regions characterized by different N_{eff} regimes look rather similar to one another (i.e., the NE Pacific, SE Pacific, and ITCZ/SPCZ). The moderate N_{eff} regimes (middle row of Fig. 12) tend to have a smaller LWP range than other regimes, whereas the Gulf of Mexico and Asian Coast have very large ranges of both LWP and N_{eff} .

Finally, even though the total drizzle frequency for a particular region can be recovered by taking the mean of all contours, the visual area of the 90% contour in a particular region provides a good sense of the drizzle frequency. This 90% contour spans a very large area in the ITCZ and SPCZ, a region where the vast majority of the screened clouds drizzle (84%), but the 90% contour only spans a tiny portion of the far SE Pacific, where the drizzle frequency of screened clouds is only 23%. The fact that the relationship among drizzle frequency, LWP, and N_{eff} is essentially the same for all regions

suggests a near universality among tropical and subtropical regions. In a given location, the distribution of LWP and N_{eff} is sufficient to predict overall drizzle frequency.

9. Summary and conclusions

This study has exploited a unique opportunity to utilize collocated passive radiometer optical parameter retrievals from MODIS with *CloudSat* radar reflectivity measurements from the A-Train system to better understand and characterize the macrophysical and microphysical factors of warm marine clouds associated with precipitation across a large part of the tropics and subtropics. We have seen that the macrophysical variables of cloud-top height and LWP are closely related, which is expected if cloud base is nearly constant. For a given cloud-top height, however, warm clouds in more polluted regions tend to have more cloud liquid water than pristine clouds. Maps of r_e and N_{eff} demonstrate that these two variables are strongly negatively correlated, and while warm cloud r_e is generally large and N_{eff} is small across the remote marine areas, droplets are smaller and concentrations much larger where continental aerosol influences become more likely, such as off the Asian coast, over the Gulf of Mexico, and in close proximity to the western South American coast and near Baja California in the far NE Pacific. Cloud-top height and LWP both tend to mirror the lower tropospheric stability rather well, with strong capping temperature inversions having the impact of restricting vertical cloud growth. Static stability is high and cloud tops shallow in the far SE Pacific and far NE Pacific, and to a lesser extent along the equatorial cold tongue. Shallow warm clouds also drizzle much less frequently than deeper warm clouds.

This study also examines macrophysical/microphysical-dBZ relationships for eight separate tropical and subtropical regions. When the maximum reflectivity in a profile is larger than -15 dBZ, drizzle drops are present in the cloud, and reflectivity values above this threshold are proportional to drizzle intensity. Cloud-top height and LWP increase substantially as drizzle intensity increases in all areas, although for a given drizzle intensity, substantially more cloud liquid water is present both near the Asian coast and over the Gulf of Mexico. These two regions also stand out as having much higher values of N_{eff} for a given dBZ, although concentrations rapidly decrease with drizzle intensity. It thus seems that drizzle intensity is more sensitive to N_{eff} when the microphysical variability in a particular region is large. In remote marine regions, the N_{eff} range is quite small, and while it plays a role in the likelihood of drizzle, it is much less important in controlling drizzle amount. Droplet radius

also tends to level off as $\text{dBZ} > 0$ in most regions, although the increase in droplet size is monotonic with dBZ over the Asian coast and the Gulf of Mexico, the more polluted of the eight regions.

Also, although drizzle frequency tends to be somewhat sensitive to N_{eff} , drizzle intensity and N_{eff} are only weakly related except in regions such as the Asian coast and Gulf of Mexico, where large background concentrations are present, and N_{eff} sharply decreases as drizzle intensity increases. It may be that the microphysics is important for drizzle rate when transitioning from a high N_{eff} , high LWP regime to lower N_{eff} . When N_{eff} is fairly low to begin with, a droplet concentration reduction may only have little influence on drizzle intensity. This behavior is reproduced in simple heuristic models, described in Part II of this study, and is fundamentally linked to the dominance of accretion, a macrophysically limited process, in generating rainwater in clouds with high LWP.

This study also examines the controlling mechanisms behind drizzle frequency. Cloud-top height appears to be the best single variable in any region in explaining the likelihood of drizzle-sized drops. Cloud LWP is also a good predictor of drizzle probability, although relationships are slightly less tight than cloud-top height among the eight different regions. When drizzle frequency is calculated as a function of both LWP and N_{eff} , drizzle probability is very likely (greater than 90%) when LWP is high and N_{eff} is low, and this is even seen in regions where overall drizzle frequency is very low, such as the far SE Pacific. Although drizzle frequency contours are slightly different in the different regions because of static stability and cloud-top height differences, these results reflect the macro- and microphysical conditions most favorable for warm rain initiation.

Acknowledgments. This work was supported by NASA Grants NNG05GA19G and NNX08AG91G. The authors thank Sandra Yuter and two anonymous referees for their comments on this manuscript.

REFERENCES

- Albrecht, B. A., 1989: Aerosols, cloud microphysics, and fractional cloudiness. *Science*, **245**, 1227–1230.
- , C. W. Fairall, D. W. Thomson, A. B. White, J. B. Snider, and W. H. Schubert, 1990: Surface-based remote sensing of the observed and the adiabatic liquid water content of stratocumulus clouds. *Geophys. Res. Lett.*, **17**, 89–92.
- Bennartz, R., 2007: Global assessment of marine boundary layer cloud droplet number concentration from satellite. *J. Geophys. Res.*, **112**, D02201, doi:10.1029/2006JD007547.
- Brenguier, J.-L., H. Pawlowska, L. Schüller, R. Preusker, J. Fischer, and Y. Fouquart, 2000: Radiative properties of boundary layer clouds: Droplet effective radius versus number concentration. *J. Atmos. Sci.*, **57**, 803–821.
- Bréon, F. M., D. Tanré, and S. Generoso, 2002: Aerosol effect on cloud droplet size monitored from satellite. *Science*, **295**, 834–838.
- Bretherton, C. S., and M. C. Wyant, 1997: Moisture transport, lower-tropospheric stability, and decoupling of cloud-topped boundary layers. *J. Atmos. Sci.*, **54**, 148–167.
- Charlson, R. J., J. E. Lovelock, M. O. Andreae, and S. G. Warren, 1987: Oceanic phytoplankton, atmospheric sulphur, cloud albedo, and climate. *Nature*, **326**, 655–661.
- Comstock, K. K., R. Wood, S. E. Yuter, and C. S. Bretherton, 2004: Reflectivity and rain rate in and below drizzling stratocumulus. *Quart. J. Roy. Meteor. Soc.*, **130**, 2891–2918.
- Fox, N. I., and A. J. Illingworth, 1997: The potential of a spaceborne cloud radar for the detection of stratocumulus clouds. *J. Appl. Meteor.*, **36**, 676–687.
- Frisch, A. S., C. W. Fairall, and J. B. Snider, 1995: Measurement of stratus cloud and drizzle parameters in ASTEX with a K_{α} -band Doppler radar and a microwave radiometer. *J. Atmos. Sci.*, **52**, 2788–2799.
- Geoffroy, O., J.-L. Brenguier, and I. Sandu, 2008: Relationship between drizzle rate, liquid water path and droplet concentration at the scale of a stratocumulus cloud system. *Atmos. Chem. Phys.*, **8**, 4641–4654.
- Han, Q., W. B. Rossow, and A. A. Lacis, 1994: Near-global survey of effective droplet radii in liquid water clouds using ISCCP data. *J. Climate*, **7**, 465–497.
- Hartmann, D. L., and D. A. Short, 1980: On the use of Earth radiation budget statistics for studies of clouds and climate. *J. Atmos. Sci.*, **37**, 1233–1250.
- Hindman, E. E., P. V. Hobbs, and L. F. Radke, 1977: Cloud condensation nucleus size distributions and their effects on cloud droplet size distributions. *J. Atmos. Sci.*, **34**, 951–956.
- Houze, R. A., 1993: *Cloud Dynamics*. Academic Press, 573 pp.
- Jensen, M. P., A. M. Vogelmann, W. D. Collins, G. J. Zhang, and E. P. Luke, 2008: Investigation of regional and seasonal variations in marine boundary layer cloud properties from MODIS observations. *J. Climate*, **21**, 4955–4973.
- King, M. D., S.-C. Tsay, S. Platnick, M. Wang, and K.-N. Liou, 1997: Cloud retrieval algorithms for MODIS: Optical thickness, effective particle radius, and thermodynamic phase. MODIS Algorithm Theoretical Basis Doc. ATBD-MOD-05, 83 pp.
- Klein, S. A., and D. L. Hartmann, 1993: The seasonal cycle of low stratiform clouds. *J. Climate*, **6**, 1587–1606.
- Kubar, T. L., and D. L. Hartmann, 2008: Vertical structure of tropical oceanic convective clouds and its relation to precipitation. *Geophys. Res. Lett.*, **35**, L03804, doi:10.1029/2007GL032811.
- Leon, D. C., Z. Wang, and D. Liu, 2008: Climatology of drizzle in marine boundary layer clouds based on 1 year of data from CloudSat and Cloud-Aerosol Lidar and Infrared Pathfinder Satellite Observations (CALIPSO). *J. Geophys. Res.*, **113**, D00A14, doi:10.1029/2008JD009835.
- Liu, Y., B. Geerts, M. Miller, P. Daum, and R. McGraw, 2008: Threshold radar reflectivity for drizzling clouds. *Geophys. Res. Lett.*, **35**, L03807, doi:10.1029/2007GL031201.
- Mace, G., 2007: Level 2 GEOPROF product process description and interface control document algorithm version 5.3, NASA Jet Propulsion Laboratory, 44 pp.
- Martin, G. M., D. W. Johnson, and A. Spice, 1994: The measurement and parameterization of effective radius and droplets in warm stratocumulus clouds. *J. Atmos. Sci.*, **51**, 1823–1842.
- Matrosov, S. Y., T. Uttal, and D. A. Hazen, 2004: Evaluation of radar reflectivity-based estimates of water content in stratiform marine clouds. *J. Appl. Meteor.*, **43**, 405–419.

- Miles, N. L., J. Verlinde, and E. E. Clothiaux, 2000: Cloud droplet size distributions in low-level stratiform clouds. *J. Atmos. Sci.*, **57**, 295–311.
- Nakajima, T., and M. D. King, 1990: Determination of the optical thickness and effective particle radius of clouds from reflected solar radiation measurements. Part I: Theory. *J. Atmos. Sci.*, **47**, 1878–1893.
- Nakajima, T. Y., and T. Nakajima, 1995: Wide-area determination of cloud microphysical properties from NOAA AVHRR measurements for FIRE and ASTEX regions. *J. Atmos. Sci.*, **52**, 4043–4059.
- Neibuhrer, M., D. S. Johnson, and C. W. Chien, 1961: The inversion over the eastern North Pacific Ocean. *Studies of the Structure of the Atmosphere over the Eastern Pacific Ocean in Summer*, Vol. I, University of California Press, 1–94.
- Pawlowska, H., and J.-L. Brenguier, 2003: An observational study of drizzle formation in stratocumulus clouds for general circulation model (GCM) parameterizations. *J. Geophys. Res.*, **108**, 8630, doi:10.1029/2002JD002679.
- Petty, G. W., 2006: *A First Course in Atmospheric Radiation*. 2nd ed. Sundog, 459 pp.
- Rauber, R. M., and Coauthors, 2007: Rain in shallow cumulus over the ocean: The RICO campaign. *Bull. Amer. Meteor. Soc.*, **88**, 1912–1928.
- Riehl, H., T. C. Yeh, J. S. Malkus, and N. E. LaSeur, 1951: The northeast trade of the Pacific Ocean. *Quart. J. Roy. Meteor. Soc.*, **77**, 598–626.
- Rogers, R. R., and M. K. Yau, 1989: *A Short Course in Cloud Physics*. 3rd ed. Butterworth Heinemann, 290 pp.
- Slingo, A., 1990: Sensitivity of the Earth's radiation budget to changes in low clouds. *Nature*, **343**, 49–51.
- Squires, P., 1956: The microstructure of cumuli in maritime and continental air. *Tellus*, **8**, 443–444.
- , 1958: The microstructure and colloidal stability of warm clouds. Part I: The relation between structure and stability. *Tellus*, **10**, 256–262.
- Stephens, G. L., and J. M. Haynes, 2007: Near global observations of the warm rain coalescence process. *Geophys. Res. Lett.*, **34**, L20805, doi:10.1029/2007GL030259.
- , and Coauthors, 2002: The CloudSat mission and the A-Train: A new dimension of space-based observations of clouds and precipitation. *Bull. Amer. Meteor. Soc.*, **83**, 1771–1790.
- , and Coauthors, 2008: CloudSat mission: Performance and early science after the first year of operation. *J. Geophys. Res.*, **113**, D00A18, doi:10.1029/2008JD009982.
- Suzuki, K., and G. L. Stephens, 2008: Global identification of warm cloud microphysical processes with combined use of A-Train observations. *Geophys. Res. Lett.*, **35**, L08805, doi:10.1029/2008GL033590.
- Szczodrak, M., P. H. Austin, and P. B. Krummel, 2001: Variability of optical depth and effective radius in marine stratocumulus clouds. *J. Atmos. Sci.*, **58**, 2912–2926.
- Twomey, S., 1974: Pollution and the planetary albedo. *Atmos. Environ.*, **8**, 1251–1256.
- , 1977: The influence of pollution on the shortwave albedo of clouds. *J. Atmos. Sci.*, **34**, 1149–1152.
- vanZanten, M. C., B. Stevens, G. Vali, and D. H. Lenschow, 2005: Observations of drizzle in nocturnal marine stratocumulus. *J. Atmos. Sci.*, **62**, 88–106.
- Wilcox, E. M., Harshvardhan, and S. Platnick, 2009: Estimate of the impact of absorbing aerosol over land on the MODIS retrievals of cloud optical thickness and effective radius using two independent retrievals of liquid water path. *J. Geophys. Res.*, **114**, D05210, doi:10.1029/2008JD010589.
- Wood, R., 2005: Drizzle in stratiform boundary layer clouds. Part II: Microphysical aspects. *J. Atmos. Sci.*, **62**, 3034–3050.
- , 2006a: Rate of loss of cloud droplets by coalescence in warm clouds. *J. Geophys. Res.*, **111**, D21205, doi:10.1029/2006JD007553.
- , 2006b: Relationships between optical depth, liquid water path, droplet concentration, and effective radius in adiabatic layer cloud. University of Washington, 3 pp. [Available online at http://www.atmos.washington.edu/~robwood/papers/chilean_plume/optical_depth_relations.pdf.]
- , and C. S. Bretherton, 2004: Boundary layer depth, entrainment, and decoupling in the cloud-capped subtropical and tropical marine boundary layer. *J. Climate*, **17**, 3576–3588.
- , T. L. Kubar, and D. L. Hartmann, 2009: Understanding the importance of microphysics and macrophysics for warm rain in marine low clouds. Part II: Heuristic models of rain formation. *J. Atmos. Sci.*, 2973–2990.
- Wu, D., Y. Hu, M. P. McCormick, K.-M. Xu, Z. Liu, B. Smith, A. H. Omar, and F.-L. Chang, 2008: Deriving marine-boundary-layer lapse rate from collocated CALIPSO, MODIS, and AMSR-E data to study low-cloud height statistics. *IEEE Geosci. Remote Sens. Lett.*, **5**, 649–652.
- Zuidema, P., E. R. Westwater, C. Fairall, and D. Hazen, 2005: Ship-based liquid water path estimates in marine stratocumulus. *J. Geophys. Res.*, **110**, D20206, doi:10.1029/2005JD005833.